



Accepted Article

Title: Spin-State Dependent Redox Catalytic Activity of a Switchable Iron(II) Complex

Authors: Il'ya A. Gural'skiy, Sergii I. Shylin, Vadim Ksenofontov, and Wolfgang Tremel

This manuscript has been accepted after peer review and appears as an Accepted Article online prior to editing, proofing, and formal publication of the final Version of Record (VoR). This work is currently citable by using the Digital Object Identifier (DOI) given below. The VoR will be published online in Early View as soon as possible and may be different to this Accepted Article as a result of editing. Readers should obtain the VoR from the journal website shown below when it is published to ensure accuracy of information. The authors are responsible for the content of this Accepted Article.

To be cited as: *Eur. J. Inorg. Chem.* 10.1002/ejic.201700454

Link to VoR: <http://dx.doi.org/10.1002/ejic.201700454>

FULL PAPER

Spin-State Dependent Redox Catalytic Activity of a Switchable Iron(II) Complex

Il'ya A. Gural'skiy,^{*[ab]} Sergii I. Shylin,^[ab] Vadim Ksenofontov^[a] and Wolfgang Tremel^[a]

Abstract: The spin state of catalytically active 3d metal centers plays a significant role for their activity in enzymatic processes and organometallic catalysis. Here we report on the catalytic activity of a Fe(II) coordination compound that can undergo a cooperative switch between low-spin (LS) and high-spin (HS) states. Catalytic measurements within 291 – 318 K temperature region reveal a drastic drop of the catalytic activity upon conversion of metallic centers from the LS to the HS form. For a thermoswitchable $[\text{Fe}(\text{NH}_2\text{trz})_3]\text{Br}_2$ complex ($T_{\text{up}} = 305 \text{ K}$), an activation energy is found to be considerably lower for the LS state (158 kJ mol^{-1}) comparing to the HS state (305 kJ mol^{-1}). Mössbauer analysis reveals that this is related to a higher conversion of a LS complex upon oxidation. The comparisons with another polymorph of $[\text{Fe}(\text{NH}_2\text{trz})_3]\text{Br}_2$ ($T_{\text{up}} = 301 \text{ K}$) and with $[\text{Fe}(\text{NH}_2\text{trz})_3](\text{ClO}_4)_2$ ($T_{\text{up}} = 240 \text{ K}$) are made. These results show the perspective of spin-crossover compounds to compare a catalytic activity of different spin states within the same material when other differentiations are minimized.

Introduction

The spin states of metals in transition metal complexes and the active sites of enzymes are in the focus of (bio) inorganic chemistry, catalysis and materials science as determinants of their magnetic properties and chemical reactivity.^[1] The coordination chemistry and the variable oxidation states of transition metals provide the mechanistic machinery for a multitude of metal-catalyzed transformations.^[2] For reactions involving paramagnetic intermediates and proceeding to form radical intermediates it is likely that the spin states of reacting intermediates (and spin-orbit coupling effects) require consideration.^[3] This is particularly relevant in biological oxidation catalysis which involves high-valent manganese^[4] or iron^[5] intermediates with variable spin states depending on the co-ligands involved, but also in chemical catalysis,^[6] where 3d metals become increasingly important and have attracted theoretical and experimental attention.^[1]

A typical example are alpha-diimine iron atom transfer radical polymerization (ATRP) catalysts, where the metal spin state correlates with the polymerization mechanism.^[7] For high-spin Fe(III) species ($S = 5/2$), living atom transfer radical polymerization predominates, whereas for catalysts in an intermediate spin state ($S = 3/2$) an organometallic pathway has led to catalytic chain transfer.^[8] It has been shown that spin transitions between HS and LS states play a key role in β -hydride elimination reactions of high-spin alkyl complexes. This leads to a spin-accelerated mechanism with the transition state having a lower-spin electronic configuration than both reactants and products.

Metals are required to circumvent spin restrictions imposed for reactions of triplet oxygen with singlet organic molecules.^[9] Thus Nature uses transition metals in different spin states to practice catalytic oxidation chemistry on a large scale, examples being Mn-catalyzed water oxidation to evolve O_2 ^[10] or the activation of carbon hydrogen bonds involving the heme-containing enzymes cytochrome P450^[11] and chloroperoxidase.^[12] Here, the electronic structures and spin states of heme-related Fe-porphyrins are crucial determinants of their reactivity.^[13]

Iron compounds are well known for their catalytic activity with iron intermediates in high oxidation states.^[14] Our approach to probe the effect of spin state on the catalytic activity was to use Fe(II) complexes that can exist in both, low-spin (LS) and high-spin (HS) states depending upon external triggers such as temperature, pressure or external fields.^[15–18] This spin crossover (SCO) effect resulting from an equilibrium of high- and low-spin states is the prototype of a switchable molecular solid with applications in molecular electronics,^[19,20] actuating devices,^[21,22] displays,^[23] microthermometry,^[24,25] and chemical sensing^[26] in solid state and coordination chemistry, biochemistry, geology, and mineralogy.^[27,28]

Results and Discussion

In order to observe the effect of spin state on the catalytic activity of iron complexes in toluene suspensions we have studied the redox catalytic activity of tris(μ_2 -4-amino-1,2,4-triazole)iron(II) bromide $[\text{Fe}(\text{NH}_2\text{trz})_3]\text{Br}_2$ ($\text{NH}_2\text{trz} = 4\text{-amino-1,2,4-triazole}$) **1** – a one-dimensional coordination polymer built up from iron-triazole chains with bromide anions situated in the inter-chain channels.^[29,30] Members of the family of Fe(II)-triazole complexes are known for their spin crossover behavior at or close to ambient temperature.^[31,32] $[\text{Fe}(\text{NH}_2\text{trz})_3]\text{Br}_2$ displays a hysteretic spin transition around room temperature. The exact transition temperature strongly depends on the synthetic procedure. Two samples of $[\text{Fe}(\text{NH}_2\text{trz})_3]\text{Br}_2$ prepared from water (**1a**) or ethanol (**1b**) were used for further investigations.

[a] Dr. I.A. Gural'skiy, S.I. Shylin, Dr. V. Ksenofontov, Prof. W. Tremel
Institute of Inorganic and Analytical Chemistry
Johannes Gutenberg University of Mainz
Duesbergweg 10-14, Mainz 55099, Germany
E-mail: illia.guralskiy@univ.kiev.ua

[b] Dr. I.A. Gural'skiy, S.I. Shylin
Department of Chemistry
Taras Shevchenko National University of Kyiv
Volodymyrska St. 64, Kyiv 01601, Ukraine

Supporting information for this article is given via a link at the end of the document.

FULL PAPER

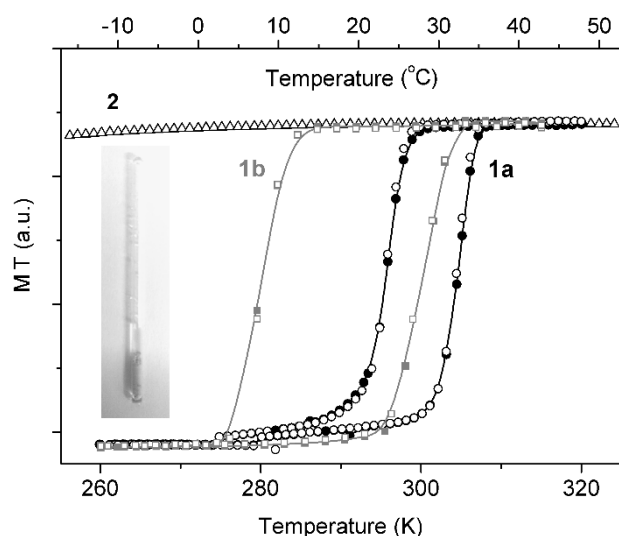
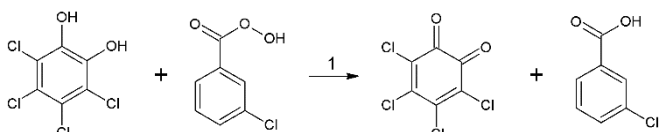


Figure 1. Temperature-dependent magnetic properties of $[\text{Fe}(\text{NH}_2\text{trz})_3]\text{Br}_2$ (**1a** and **1b**) and $[\text{Fe}(\text{NH}_2\text{trz})_3](\text{ClO}_4)_2$ (**2**) in toluene. **1a** and **1b** show spin-crossover behavior between 260 and 320 K, whereas **2** does not change its spin state. A photograph of the capillary with sample is inserted. Magnetization is given in arbitrary units. It was not turned in molar units since precise values cannot be obtained for a very elongated capillary with a liquid diamagnetic toluene inside.



Scheme 1. Model redox reaction to demonstrate the redox catalytic activity of $[\text{Fe}(\text{NH}_2\text{trz})_3]\text{Br}_2$.

The spin behavior of the complexes was monitored (in closed capillaries under liquid toluene, **Figure S1**) by SQUID magnetometry (**Figure 1**). **1a** and **1b** displayed a cooperative spin transition around room temperature (**1a**: $T_{\text{up}} = 305$ K, $T_{\text{down}} = 296$ K; **1b**: $T_{\text{up}} = 301$ K, $T_{\text{down}} = 283$ K). These temperatures are similar to those firstly reported for this complex by L.G. Lavrenova et al. in 1990 ($T_{\text{up}} = 312$ K, $T_{\text{down}} = 302$ K for the hydrated form; $T_{\text{up}} = 302$ K, $T_{\text{down}} = 284$ K for the dehydrated form).^[29] PXRD patterns of two isomorphous forms obtained by us are given in **Figure S2**. For comparison we used the analogous complex $[\text{Fe}(\text{NH}_2\text{trz})_3](\text{ClO}_4)_2$ (**2**) containing a perchlorate counter anion which has no spin transition in the given temperature range (LS→HS transition occurs at ~ 240 K, **Figure S3**). 3,4,5,6-tetrachlorocatechol (TCC) was used as substrate because its oxidation product (3,4,5,6-tetrachloro-1,2-chinone, **Figure S4**) could easily be detected spectrophotometrically (**Scheme 1**). The oxidizing agent was 3-chloroperoxybenzoic acid (CPBA) in toluene. Nonpolar toluene was specifically used to avoid any dissolution (solvolysis) of the iron complexes. Tetrachloroquinone shows a specific adsorption band at 390 nm (**Figure 2a**) that was used to monitor the progress of the reaction by UV-Vis

spectroscopy. TCC and CPBA do not absorb at 390 nm (**Figure S5**). Without catalyst the reaction is very slow and takes hours, whereas the catalytic reaction may occur within seconds.

The kinetic curves for this model reaction for different quantities of **1a** in **Figure 2a** demonstrate a pronounced catalytic efficiency of the Fe(II)-triazole complex in the solid state, i.e. the reaction was carried out in a heterogeneous fashion. The reaction was zeroth order for catechol, whereas the rate depends on the catalyst concentration. For identical starting concentrations of catechol and peroxide dA/dt grows linearly with the catalyst concentration (**Figure 2b**). For a given precursor concentration the reaction follows a pseudo-zeroth order kinetics that can be summarized as

$$\frac{dc_{\text{chinone}}}{dt} = \frac{dA_{\text{chinone}}}{(\epsilon l)dt} = k_{\text{eff}} \quad (1)$$

where ϵ is the molar extinction of the chinone, l the optical pathlength, and k_{eff} the effective rate constant.

To demonstrate the SCO effect on the catalytic activity of **1a**, we studied the temperature dependent kinetics for the reaction between 18 and 45 °C. The corresponding kinetic curves are displayed in **Figure 3a**. Conversion after 1 min in the reactions carried out at different temperatures are shown in **Figure 3b**. All reactions are pseudo-zeroth order in catechol irrespective of the temperature.

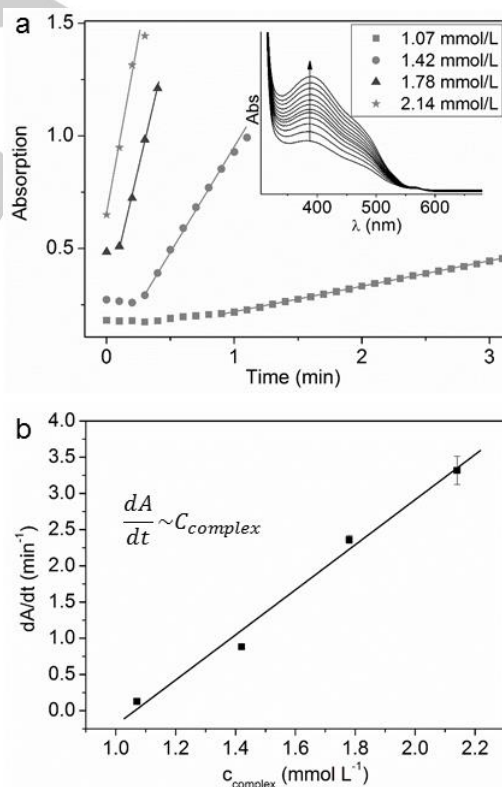


Figure 2. Catalytic effect of $[\text{Fe}(\text{NH}_2\text{trz})_3]\text{Br}_2$ on the kinetics of the TCC oxidation at 39 °C. (a) Kinetic curves for different concentrations of **1a**. The insert shows the evolution of the UV-Vis spectrum upon catechol conversion. (b) Conversion rate as a function of the catalyst concentration.

FULL PAPER

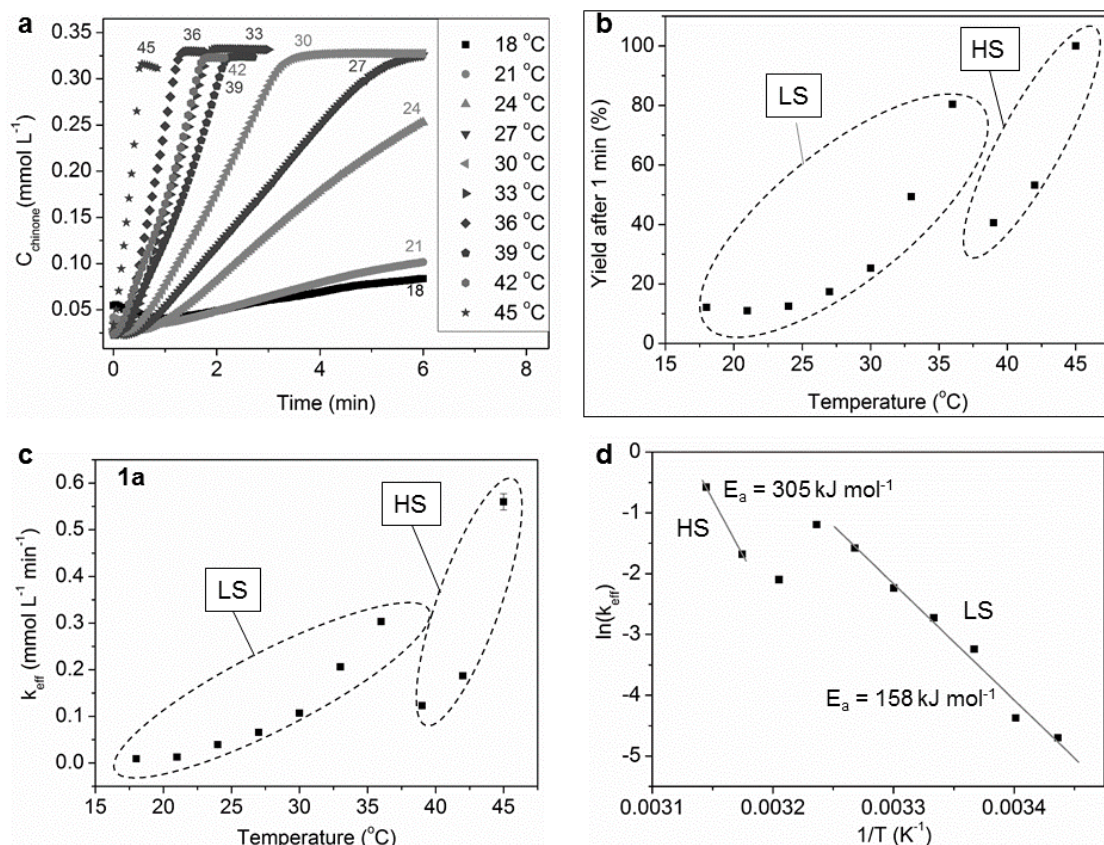


Figure 3. Effect of a spin state on the catalytic activity in the reaction of TCC oxidation ($C_{\text{TCC}} = 0.309 \text{ mM}$, $C_{\text{CPBA}} = 4.48 \text{ mM}$, $C_{\text{complex}} = 2.14 \text{ mM}$). (a) Kinetic curves of TCC oxidation catalyzed by **1a** at different temperatures within 18–45 °C region. (b) Yield of tetrachloroquinone after 1 min of reactions conducted at different temperatures. (c) Dependence of the reaction rate constant on temperature. (d) Arrhenius plot demonstrates the presence of two kinetic regimes for different spin states of the catalyst.

Final concentration of tetrachloroquinone (concentration on plateau) is the same for all reactions made at different temperatures (~0.32–0.36 mmol L^{-1}). This compound can be considered as a principal oxidation product (intermediate) which is stable in the timeframes of these reactions, that is why its concentration was monitored here. It should be noted that this quinone may undergo further condensation and dechlorination transformations. These following transformations of tetrachloroquinone are responsible for the gradual decrease of its concentration after reaching the plateau, with a pronounceable slope observed at elevated temperatures (see 45 °C curve in **Figure 3a**).

The rate constants k_{eff} vs. temperature (extracted from the gradients) are shown in **Figure 3c**, and the temperature-dependence of rate constants according to

$$\ln(k_{\text{eff}}) = \ln(A) - \frac{E_a}{R} \frac{1}{T} \quad (2)$$

is given in **Figure 3d**, with A as pre-exponential factor, R the universal gas constant, and E_a as activation energy.

The reaction rate shows Arrhenius behavior and gradually increases with temperature between 18 and 36 °C. A drastic drop of the catalytic activity at 36 °C is associated with the SCO.

After the change of spin state was complete, the temperature dependence between 39 °C and 45 °C showed Arrhenius behavior again. In essence, **Figure 3** clearly differentiates two distinct temperature regions associated with the $\text{Fe}^{\text{II}}(\text{HS})$ and $\text{Fe}^{\text{II}}(\text{LS})$ states of **1a**. Using **Equation 2** the activation energies for the spin states could be extracted as $E_a^{\text{LS}} = 158(11) \text{ kJ mol}^{-1}$ and $E_a^{\text{HS}} = 305 \text{ kJ mol}^{-1}$. This abrupt increase corroborates with the observation that the LS state was more active than the HS state. Its origin is assumed to be related to the electronic structures of two forms and may be due to differences in the electronic multiplicity, redox potential, lattice energies, etc.

To confirm the effect of SCO on this redox reaction, we carried out analogous experiments with **1b** ($[\text{Fe}(\text{NH}_2\text{trz})_3]\text{Br}_2$ (precipitated from ethanol rather than from water) that displayed a lower transition temperature than **1a** (**Figure 1**). Rate constants as a function of temperature are shown in **Figure 4a**. The most important conclusion is that the effect of the spin transition on this reaction was observed as well. The reaction rate followed an Arrhenius behavior between 23 °C and 29 °C and showed a pronounced drop after the SCO.

FULL PAPER

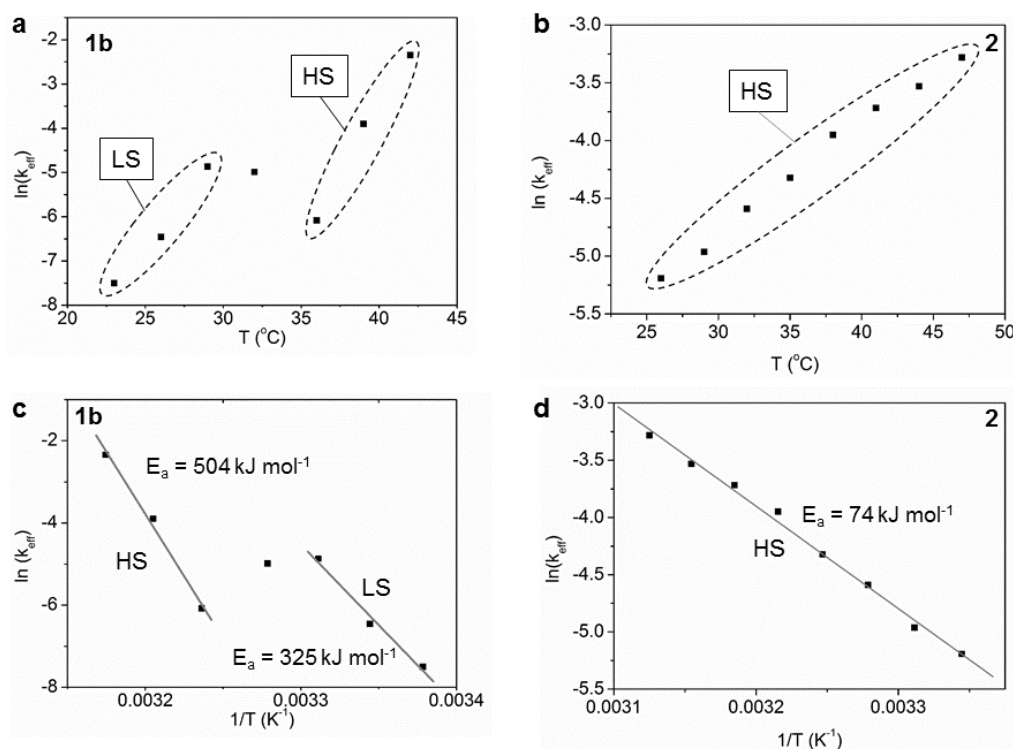


Figure 4. Temperature-dependent catalytic activity of Fe(II)-triazolic complexes ($C_{TCC} = 0.309$ mM, $C_{CPBA} = 4.48$ mM, $C_{1b} = 2.1$ mM, $C_2 = 2$ mM). (a) Rate constants of TCC oxidation catalyzed by **1b** at different temperatures within 23–42 °C. (b) Rate constants of TCC oxidation catalyzed by **2** at different temperatures within 26–47 °C. (c) Arrhenius plot for the oxidation catalyzed by **1b** demonstrates an effect of spin state on the catalytic activity. (d) Arrhenius plot for the oxidation catalyzed by a HS complex **2** demonstrates a classical dependence of the reaction rate on temperature.

The simultaneous presence of the Fe^{II}(HS) and Fe^{II}(LS) states in the spin equilibrium range around 32 °C leads to a superposition of the reactivities of both states in **Figure 3** (for **1a**) and **Figure 4** (for **1b**). After the transition was complete for **1b** at 36 °C the reaction rate increased again in an Arrhenius-type manner. This sudden change in the reaction rate agrees with the transition temperature of **1b** (a systematic shift related to the thermalization in kinetic experiments should be considered when comparing with magnetic measurements). The slight difference in the temperature of the “activity drop” for **1a** and **1b** is assumed to be related to the different transition temperatures.

Even more informative is the comparison with a sample that displays no spin transition. We have synthesized **2** that contains iron-triazole chains as **1a** and **1b**, but the chains are separated by perchlorate rather than bromide anions. As a result, **2** adopts the HS state in toluene suspension above room temperature (**Figure 1**).

The activation energies of $E_a^{LS} = 325(41)$ kJ mol⁻¹ and $E_a^{HS} = 504(46)$ kJ mol⁻¹ derived for the LS and HS states **1b** (**Figure 4c**) are slightly higher than those for **1a**; comparison of HS and LS activation energies indicates that the LS state is more reactive than the HS state. Complex **2** showed Arrhenius behavior (**Figure 4d**) without deviations from linearity. The activation energy $E_a^{HS} = 74(2)$ kJ mol⁻¹ was small and lower than that observed for the LS and HS states of **1a** and **1b**.

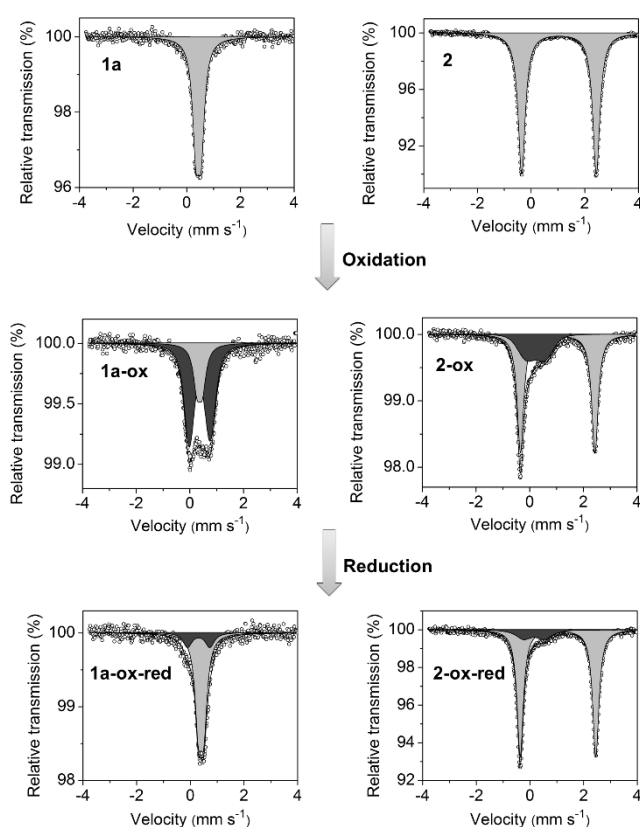
To understand this difference in the catalytic activity, we have analyzed the tendency of the two spin states to be oxidized,

because iron in high valence states is assumed to play a crucial role as intermediate. Mössbauer spectroscopy is the most convenient way to monitor the relative amounts of iron in different oxidation and spin states in solid samples.^[33] Mössbauer spectra of **1a** and **2** have hyperfine parameters very well corroborating with those obtained by Lavrenova et al.^[29] We recorded Mössbauer spectra of **1a** and **2** that were treated with an excess of CPBA to achieve a partial (but considerable) oxidation of **1a** and **2** (named **1a-ox** and **2-ox**). Moreover, a reduction by TCC was used to reduce iron to its initial form (**1a-ox-red** and **2-ox-red**) and thus reproduce a whole catalytic cycle. Mössbauer spectra of precursors and oxidized samples are shown in **Figure 5**. Each oxidized sample contains iron in Fe(II) and Fe(III) oxidation states (oxidized form can be different within a catalytic cycle, e.g. Fe(IV) frequently plays a role of an intermediate). Their principal hyperfine parameters are summarized in **Table 1**. Oxidation does not affect the spin state of Fe(II) centers. In its order, the oxidation state of newly formed Fe(III) centers is hardly definable just from hyperfine parameters.^[34] What is also important, TCC can majorly reduce these Fe(III) fractions back to initial Fe(II) forms (samples **1a-ox-red** and **2-ox-red**) as shown in **Figure 5**. Complex **1a** used for the kinetic measurements does not show any considerable content of the oxidized form after one catalytic cycle (**Figure S8**).

FULL PAPER

Table 1. Mössbauer hyperfine parameters of **1a**, **2**, **1a-ox** and **2-ox**. A higher conversion to Fe^{III} is displayed by a HS complex comparing to a LS complex ($C_{TCC} = 300$ mM, $C_{CPBA} = 130$ mM, $C_{complex} = 20$ mM).

	Reduced form (Fe ^{II})				Oxidized form (Fe ^{III})		
	Content (%)	Spin state	δ (mm s ⁻¹)	ΔE_Q (mm s ⁻¹)	Content (%)	δ (mm s ⁻¹)	ΔE_Q (mm s ⁻¹)
[Fe(NH ₂ trz) ₃]Br ₂ (1a)	100	LS	0.436(3)	0.207(7)			
[Fe(NH ₂ trz) ₃](ClO ₄) ₂ (2)	100	HS	1.041(2)	2.781(5)			
1a-ox	25(3)	LS	0.37(1)	0.2(fixed)	75(3)	0.37(1)	0.78(2)
2-ox	71.0 (8)	HS	1.04(1)	2.78(2)	29.0(8)	0.22(1)	0.73(2)
1a-ox-red	82(3)	LS	0.40(1)	0.21(2)	18(5)	0.31(2)	0.79(3)
2-ox-red	85(1)	HS	1.044(1)	2.818(3)	15(2)	0.19(4)	0.77(6)

**Figure 5.** Mössbauer spectra of **1a** and **2**, their oxidized (**1a-ox** and **2-ox**) and newly reduced (**1a-ox-red** and **2-ox-red**) forms. Fe(II) species are shown in gray and Fe(III) are shown in black. The content of the Fe(III) species reflects a higher conversion of LS Fe(II) (vs. HS Fe(II)) upon oxidation.

When using model peroxidase substrates instead of TCC, e.g. 3,3',5,5'-tetramethylbenzidine or 2,2'-azino-bis(3-ethylbenzothiazoline-6-sulphonic acid), triazolic complexes do not display any catalytic activity that excludes a peroxidase-like mechanism. We believe that the studied catalytic cycle has two principal steps: (i) oxidation of the iron complex by peroxyacid and (ii) reduction of the complex by TCC. As revealed by Mössbauer measurements, both of these steps can be reproduced separately. The higher catalytic activity of the LS species can reasonably be referred to their higher inclination towards oxidation under otherwise identical conditions.

Both complexes (**1a** and **2**) undergo a partial oxidation, while the Fe(III) content is different in each case. When the **1a** in its LS state (at room temperature) is oxidized, the ferric form is present in amounts of 75(3) %. However, when **2** reacts in its HS state (at room temperature), the Fe(III) content is just 29(1) %. This considerable difference reveals that for very similar complexes, the spin state plays a prominent role in the oxidation process. This observation is in line with the results of the catalytic oxidation of TCC.

Conclusions

We have found that in the SCO compound [Fe(NH₂trz)₃]Br₂ the spin state of the Fe(II) centers plays a crucial role in determining their redox catalytic activity. The LS species are characterized by higher reaction rates and smaller activation energies compared to the HS analogues. We demonstrated that this difference is driven by a higher tendency of LS iron(II) to be oxidized. Such spin-dependent activity will be analyzed for other switchable SCO complexes and other types of chemical reactions in order to derive a broader picture of the effect of spin state on the catalytic metal centers, in particular as photochemical and electrochemical activities may be very sensitive to the spin state of the catalyst. Application of chiral switchable complexes^[35,36] may lead to a switchable stereoselectivity in catalysis.

FULL PAPER

Experimental Section

Synthesis. $[\text{Fe}(\text{NH}_2\text{trz})_3]\text{Br}_2$ (**1a**). NH_2trz (250 mg, 2.98 mmol) in water (1 mL) and FeBr_2 (210 mg, 0.97 mmol) in water (1 mL) were mixed under stirring. The precipitate was formed within 1 h and separated by centrifugation (13000 rpm, 4 min), washed with water and dried in air. Yield is 344 mg (74 %). Anal. Calcd for $\text{C}_6\text{H}_{12}\text{N}_4\text{Br}_2\text{Fe}$: C, 15.40; N, 35.92; H, 2.59. Found: C, 15.75; N, 36.12; H, 2.31. $[\text{Fe}(\text{NH}_2\text{trz})_3]\text{Br}_2$ (**1b**). The sample was obtained as described for **1a**, by replacing water with ethanol in all steps. Yield is 382 mg (82 %). Anal. Calcd for $\text{C}_6\text{H}_{12}\text{N}_4\text{Br}_2\text{Fe}$: C, 15.40; N, 35.92; H, 2.59. Found: C, 15.51; N, 35.96; H, 2.48.

$[\text{Fe}(\text{NH}_2\text{trz})_3](\text{ClO}_4)_2$ (**2**). The sample was prepared as **1a** starting from NH_2trz (250 mg, 2.98 mmol) and $\text{Fe}(\text{ClO}_4)_2 \cdot 6\text{H}_2\text{O}$ (360 mg, 0.99 mmol). Yield is 330 mg (65 %). Elemental analysis was not performed for safety reasons.

Catalysis. Catalytic measurements were performed in 3.5 mL quartz cuvettes with 1 cm optical pathway. The temperature in the cuvette holder was controlled with a Haake C50P thermostat. The concentration of the product was monitored by measuring the absorption of quinone with a UV-Vis Cary spectrometer at 390 ± 2.5 nm with a 5 sec interval.

A catalyst (3 mg) was added to the TCC (0.23 mg) in toluene (2.9 mL). The cuvette was thermalized for 4 min prior to each measurement. CPBA in toluene (0.1 mL, 0.13 mol L^{-1}) was added after and a UV-Vis monitoring started directly. No stirring during the reaction was applied.

Oxidized samples. To produce **1a-ox** and **2-ox**, a Fe(II) complex (0.1 mmol) was mixed with 3-chloroperoxybenzoic acid in toluene (3 mL, 0.13 mol L^{-1}) and allowed to stay for 5 min at 20°C . To produce **1a-ox-red** and **2-ox-red**, oxidized samples (0.1 mmol) were treated with TCC solution (3 mL, 0.3 mol L^{-1}) and allowed to stay for 5 min at 20°C . The powders were separated from solutions by centrifugation (13000 rpm, 1 min), washed with toluene and dried in air.

Magnetic susceptibility measurements. Temperature-dependent magnetic susceptibility measurements were carried out with a Quantum-Design MPMS-XL-5 SQUID magnetometer with a heating and cooling rate of 1 K min^{-1} , and a magnetic field of 0.5 T. A powder sample mixed with liquid toluene was sealed using a hydrogen torch in a glass capillary (~ 4.5 mm long, inner diameter is 1.0 mm, outer diameter is 1.4 mm). Capillary was fixed between two gelatin capsules. Molar magnetization was not calculated because of the considerable diamagnetic impact of toluene and of the capillary, which could not be accurately subtracted.

Mössbauer spectroscopy. ^{57}Fe -Mössbauer spectra were recorded in transmission geometry with a ^{57}Co source in a rhodium matrix using a conventional constant-acceleration Mössbauer spectrometer. Isomer shifts are given with respect to an α -Fe foil at ambient temperature. Fits of the experimental Mössbauer data were performed using the Recoil software (Lagarec and Rancourt, Ottawa University).

Acknowledgements

This work was financed by H2020-MSCA-IF-2014 grant 659614. We acknowledge useful commentaries from Prof. I.O. Fritsky, spectroscopic measurements from D. Spetter and graphical contribution from O.I. Kucheriv. We also acknowledge very useful comments from the anonymous reviewer on the mechanism of the studied reaction.

Keywords: iron • spin crossover • spin state • catalysis • Mössbauer spectroscopy

- [1] M. Swart, M. Costas, Eds., *Spin States in Biochemistry and Inorganic Chemistry*, John Wiley & Sons, Ltd, Oxford, UK, **2015**.
- [2] R. H. Holm, P. Kennepohl, E. I. Solomon, *Chem. Rev.* **1996**, *96*, 2239–2314.
- [3] T. Risse, D. Hollmann, A. Brückner, in *Catalysis* **2015**, *27*, 1–32.
- [4] T. Yang, M. G. Quesne, H. M. Neu, F. G. Cantú Reinhard, D. P. Goldberg, S. P. de Visser, *J. Am. Chem. Soc.* **2016**, *10.1021/jacs.6b05027*.
- [5] M. Higuchi, Y. Hitomi, H. Minami, T. Tanaka, T. Funabiki, *Inorg. Chem.* **2005**, *44*, 8810–8821.
- [6] G. Xue, R. De Hont, E. Münck, L. Que, *Nat. Chem.* **2010**, *2*, 400–405.
- [7] L. E. N. Allan, M. P. Shaver, A. J. P. White, V. C. Gibson, *Inorg. Chem.* **2007**, *46*, 8963–70.
- [8] M. P. Shaver, L. E. N. Allan, H. S. Rzepa, V. C. Gibson, *Angew. Chemie Int. Ed.* **2006**, *45*, 1241–1244.
- [9] J. S. Valentine, *Bioinorg. Chem.* **1994**, 313–523.
- [10] V. Krewald, M. Retegan, F. Neese, W. Lubitz, D. A. Pantazis, N. Cox, *Inorg. Chem.* **2016**, *55*, 488–501.
- [11] F. P. Guengerich, A. W. Munro, *J. Biol. Chem.* **2013**, *288*, 17065–17073.
- [12] M. T. Green, *J. Am. Chem. Soc.* **2006**, *128*, 1902–1906.
- [13] M. E. Ali, B. Sanyal, P. M. Oppeneer, *J. Phys. Chem. B* **2012**, *116*, 5849–5859.
- [14] A. Ghosh, D. Mitchell, A. Chanda, A. D. Ryabov, D. L. Popescu, E. C. Upham, G. J. Collins, T. J. Collins, V. Pennsly, *J. Am. Chem. Soc.* **2008**, *130*, 15116–15126.
- [15] S. Brooker, *Chem. Soc. Rev.* **2015**, *44*, 2880–2892.
- [16] M. A. Halcrow, *Spin-Crossover Materials*, John Wiley & Sons Ltd, Oxford, UK, **2013**.
- [17] P. Gütllich, *Eur. J. Inorg. Chem.* **2013**, *2013*, 581–591.
- [18] P. Gütllich, H. A. Goodwin, in *Top. Curr. Chem.*, Springer, **2004**.
- [19] J. Dugay, M. Giménez-Marqués, T. Kozlova, H. W. Zandbergen, E. Coronado, H. S. J. van der Zant, *Adv. Mater.* **2015**, *27*, 1288–1293.
- [20] A. Rotaru, J. Dugay, R. P. Tan, I. A. Gural'skiy, L. Salmon, P. Demont, J. Carrey, G. Molnár, M. Respaud, A. Bousseksou, *Adv. Mater.* **2013**, *25*, 1745–1749.
- [21] H. J. Shepherd, I. A. Gural'skiy, C. M. Quintero, S. Tricard, L. Salmon, G. Molnár, A. Bousseksou, *Nat. Commun.* **2013**, *4*, 2607.
- [22] I. A. Gural'skiy, C. M. Quintero, J. S. Costa, P. Demont, G. Molnár, L. Salmon, H. J. Shepherd, A. Bousseksou, *J. Mater. Chem. C* **2014**, *2*, 2949–2955.
- [23] O. Kahn, J. Kröber, C. Jay, *Adv. Mater.* **1992**, *4*, 718–728.
- [24] L. Salmon, G. Molnar, D. Zitouni, C. Quintero, C. Bergaud, J.-C. Micheau, A. Bousseksou, *J. Mater. Chem.* **2010**, *20*, 5499–5503.
- [25] I. A. Gural'skiy, C. M. Quintero, K. Abdul-Kader, M. Lopes, C. Bartual-Murgui, L. Salmon, P. Zhao, G. Molnar, D. Astruc, A. Bousseksou, *J. Nanophotonics* **2012**, *6*, 63513–63517.
- [26] J. A. Real, A. B. Gaspar, M. C. Muñoz, *Dalt. Trans.* **2005**, 2062.
- [27] B. Chance, *Science* **1968**, *159*, 654–658.
- [28] T. Kawakami, Y. Tsujimoto, H. Kageyama, X.-Q. Chen, C. L. Fu, C. Tassel, A. Kitada, S. Suto, K. Hiram, Y. Sekiya, Y. Makino, T. Okada, T. Yagi, N. Hayashi, K. Yoshimura, S. Nasu, R. Podloucky, M. Takano, *Nat. Chem.* **2009**, *1*, 371–376.
- [29] L. G. Lavrenova, V. N. Ikorskii, V. A. Varnek, I. M. Oglezneva, S.V. Larionov, *Koord. Khim.* **1990**, *16*, 654–661.
- [30] O. Fouché, J. Degert, G. Jonusauskas, N. Daro, J.-F. Létard and E. Freysz, *Phys. Chem. Chem. Phys.* **2010**, *12*, 3044–3052.
- [31] L. G. Lavrenova, O. G. Shakirova, *Eur. J. Inorg. Chem.* **2013**, *2013*, 670–682.
- [32] O. Roubeau, *Chem. Eur. J.* **2012**, *18*, 15230–15244.
- [33] P. Gütllich, Y. Garcia, in *Mössbauer Spectrosc.* (Eds.: Y. Yoshida, G. Langouche), Springer Berlin Heidelberg, Berlin, Heidelberg, **2013**, pp. 23–89.
- [34] F. Neese, *Inorg. Chim. Acta* **2002**, *337*, 181–192.
- [35] I. A. Gural'skiy, O. I. Kucheriv, S. I. Shylin, V. Ksenofontov, R. A. Polunin, I. O. Fritsky, *Chem. Eur. J.* **2015**, *21*, 18076–18079.

FULL PAPER

- [36] I. A. Gural'skiy, V. A. Reshetnikov, A. Szabeszcyk, E. Gumienna-Kontecka, A. I. Marynin, S. I. Shylin, V. Ksenofontov, I. O. Fritsky, *J. Mater. Chem. C* **2015**, *3*, 4737–4741.

WILEY-VCH

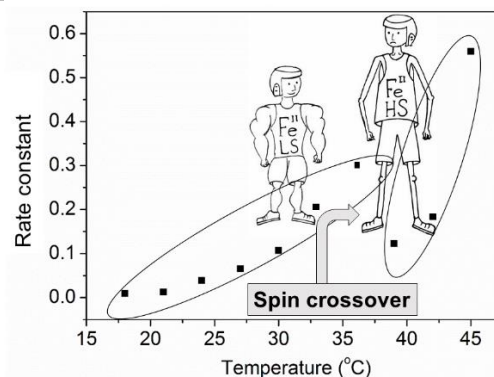
Accepted Manuscript

FULL PAPER

Entry for the Table of Contents

FULL PAPER

Spin-crossover Fe(II) complex $[\text{Fe}(\text{NH}_2\text{trz})_3]\text{Br}_2$ shows a redox catalytic activity that changes upon conversion of metallic centers from the low-spin to the high-spin form. The activation energy is considerably smaller for the low-spin state. This difference is related to a higher tendency of the diamagnetic form towards oxidation.



Il'ya A. Gural'skiy, Sergii I. Shylin, Vadim Ksenofontov and Wolfgang Tremel*

Page No. – Page No.

Spin-State Dependent Redox Catalytic Activity of a Switchable Iron(II) Complex